

ON TESTING QUALITY AND TRACEABILITY OF VIRGIN OLIVE OIL BY CALORIMETRY

M. Angiuli¹, C. Ferrari¹, L. Lepori¹, E. Matteoli¹, G. Salvetti^{1*}, E. Tombari¹,
A. Banti² and N. Minnaja²

¹Istituto per i Processi Chimico-Fisici del CNR, via G. Moruzzi 1, 56124 Pisa, Italy

²Polo Tecnologico del Gusto, 56023 Navacchio, Pisa, Italy

Extra Virgin olive oils (7 samples) originating from different areas of Tuscany, defective olive oils (5 samples), commercial edible seed oils (4 samples) and two commercial samples of olive oil (one declared 'extra virgin olive oil' and one 'olive oil') were studied by different calorimetric techniques: high sensitivity isothermal, differential scanning, and modulated scanning calorimetry. The temperature interval (–60)–(+30)°C was explored for monitoring: *i*) the main features of the liquid↔solid phase transitions, *ii*) the nucleation and growth rate of the polymorphous crystalline phases of the triacylglycerols, and *iii*) the melting process. This investigation was planned for verifying the utility and effectiveness of calorimetry for screening quality and origin of olive oil. To this end, the main calorimetric operation modes have been applied, the experimental results reported and their utility for developing an effective and reliable screening protocol discussed.

Keywords: calorimetry, olive oil, phase transitions, triacylglycerol crystallization

Introduction

Molecular components of olive oils and vegetable edible oils are mainly triacylglycerols (TAGs) mixed with other organic molecules (diacylglycerols, paraffins, fatty acids, phospholipids, phenols, etc.) [1, 2]. Owing to their complexity, they show time and temperature dependent physical properties. Among the numerous experimental techniques for studying these complex fluids [2], many researchers have suggested the use of calorimetry as a simple tool able to provide reliable information on the nature, quality, and also geographic origin of the oils. Their interest has been devoted to the features of the liquid↔solid phase transitions that reflect composition, type and size of the components, and the rate of the physical and chemical processes undergone by oil in its time-temperature history. In particular, the solidification process involves physical phenomena such as: *i*) the wax appearance at a characteristic temperature [3], *ii*) the polymorphism of the TAG crystals, dependent on the structure of the TAG molecule, *iii*) the nucleation temperature, affected by the amount of other organic molecules in the liquid oil [4].

Differential Scanning Calorimetry (DSC) is a calorimetric technique that has been commonly used [5] for these studies. DSC crystallization and melting curves show relevant features of the processes, such as the characteristic temperatures and the enthalpy.

These quantities have been correlated to the quality and the stability of the edible oils [6–9]. It must be pointed out that the richness of the curve profiles and the number of significant variables is such that Dyszel SM. of US Customs Service has worked from 1982 to 1996 for creating a data bank with the calorimetric 'fingerprints' of the main edible oils [10–12]. Other important uses of calorimetry are the study of the thermo-oxidative process [13–16], with the purpose of improving storage and utilization conditions against temperature, and for applications in analytical chemistry [17, 18].

Our research moves from this promising background with the aim of verifying the applicability of calorimetry, including all the main operative modes now at disposal, for assessing quality and traceability of the extra-virgin olive oils produced in Tuscany (Italy), in particular the presence of defects resulting both from natural degradation due to time-temperature storage history, or from adulterations and frauds.

According to European rules, the label 'extra-virgin olive oil' may be appointed to an oil bottle if a set of chemical and physical analyses and also an 'organoleptic' assessment have given satisfactory results; this latter must be provided by a panel of people trained to distinguish the peculiar tastes of good and defective oils. In fact, chemistry alone is unable to provide a reliable interpretation of the human sensations of taste and flavour, so that both types of tests

* Author for correspondence: salvetti@ipcf.cnr.it

have to be passed. Other distinctive labels may be also posted up, to indicate the origin of the oil; in this case, not only the path of the product from the tree to the bottle has to be traced, but also the results of the chemical tests have to meet tighter standards, matching the peculiar features of the oils of that particular region. To overcome the low reproducibility of organoleptic tests, the application of techniques of 'artificial intelligence' has been proposed recently, leading to an equipment and an experimental procedure known as 'artificial olfactory system', or shortly, 'electronic nose'. The first results obtained by means of this technique on the same set oils presented in this paper have been recently reported [19]. The application of calorimetry is considered a complementary or alternative way to the electronic nose for establishing the quality of olive oil in a short time and at a reasonable cost without the uncertainty of a subjective human test.

Here we report preliminary results from DSC, isothermal calorimetry and modulated temperature scanning calorimetry. The solidification process of the oil samples has been studied isothermally at 2.9°C, which is practically the temperature of the Tuscany cellars during winter, when the olive oil 'freezes' in the bottles with characteristic structures and colours, traditionally considered by country people as features correlated to the oil quality. The solid↔liquid phase transitions have been also monitored during cooling and heating cycles in a wide temperature range with both DSC and MASC, a modulated, adiabatic and temperature scanning calorimeter [20]. The modulated calorimetry gives information on the reversibility of the processes and on the polymorphism of the crystal structures. To our knowledge, it has been used previously only one time for measuring the wax appearance temperature of crude oils [21], thus we are here reporting its first application for the characterization of olive oil.

From the analysis of the collected data we will try to assess pros and cons of the use of each calorimeter and calorimetric operation mode and, finally, to suggest the most appropriate experimental technique and measuring procedure for a reliable screening of olive oil identity.

Experimental

Materials

The olive oil samples have been supplied by the facility Polo Tecnologico del Gusto (Technological Centre for Taste), Navacchio (Pisa, Italy). They are extra-virgin oil samples and defected oils according to the judgment of a qualified panel of tasters. Con-

trolled quantities of selected single defect (rancid, vinegary, fusty) have been added to the same mother extra-virgin oil in order to build up a sensitivity scale. The several extra-virgin olive oils, from different Tuscan provinces and different cultivars, have been tested with the aim of finding differences correlated to: *i*) the predominant cultivar; *ii*) the geographic origin of the fruits; *iii*) the oil production/ storage procedures; and *iv*) the organoleptic features assessed by the panel. The samples have been supplied and maintained in sealed ampoules stored in dark at 18°C. Moreover few commercial seed oils and one 'extra-virgin olive oil' and one declared 'olive oil' have been tested for comparison. The chemical and organoleptic characteristics certified by the supplier, or the oil description as reported on the label of the commercial packet, are summarized in Table 1 for each sample.

Methods

Isothermal calorimetry

The measurements were carried out at 2.9°C with a heat-flow TAM calorimeter MOD. 2277 by Thermometric. The heat flow to or from the measuring cell, containing a quantity of oil ranging from 0.4 to 0.6 g in an atmosphere of air, was measured for 20 to 100 h, until the equilibrium conditions were attained, that is the solidification attained to completion. After the first run, the sample cell was pulled out of the calorimeter and kept at 18°C for a time ranging from 1 to 10 h to test the time necessary for a complete melting of the polymorphic structures grown in the solid sample. Then the sample cell was again loaded into the calorimeter at 2.9°C. The recording of the second run started after about half an hour, when the calorimeter had reached its baseline. The specific enthalpy of freezing was obtained by integration of the curve, after baseline subtraction. The results obtained in the two runs performed for each sample are collected in Table 2 together with the time value necessary to reach the peak of the freezing curve. The isothermal calorimetry was previously applied for studying the oxidation of lipids [22].

Modulated temperature scanning calorimetry

We have been using the home-made calorimeter MASC (Modulated Adiabatic and temperature Scanning Calorimeter) for studying the melting and freezing processes of olive oil samples with the main calorimetric operation modes (scanning, isothermal and temperature modulation). The sample, a volume of about 0.2 cm³, is contained in a Pyrex capillary tube in presence of air (about 0.1 cm³), sealed at both ends

Table 1 Characteristics of the oil samples investigated in the reported experiments

Extra virgin olive oils												
No.	Sample	Taste			Polyphenols/ mg/kg gallic acid	Acidity/ oleic acid%	N° perox./ mEO ₂ kg ⁻¹	Other features				
		Fruity	Bitter	Pungent				Origin		Cultivar		
			Median					Frantoio	Leccino	Moraiolo	Pendolino	Maurino
1	EXA16PT	4.55	2.90	4.40	96.00	0.15	9.65	Pistoia	50%	0%	0%	0%
2	EXA25F1	3.00	3.80	3.90	111.00	0.20	9.20	Firenze	50%	30%	10%	0%
3	EXA26F1	3.50	3.55	3.95	154.00	0.20	10.85	Firenze	20%	60%	0%	0%
4	EXA27GR	5.50	6.45	5.30	116.00	0.15	11.35	Grosseto	34%	30%	3%	3%
5	EXA28GR	4.55	4.05	5.35	105.00	0.15	10.15	Grosseto	90%	0%	10%	0%
6	EXA31SI	4.75	4.05	5.35	119.00	0.15	8.55	Siena	62%	20%	15%	3%
Defective olive oils												
No.	Sample	Added defect			Acidity/ oleic acid%	N° perox./ mEO ₂ kg ⁻¹	No.	Commercial edible oils				
		Vinegary	Rancid	oleic acid%				Declared on the label				
7	EXA1SI	0%	0%	0%	0.15	8.55	13	Extra virgin olive oil				
8	EXA1SI	1.20%	0%	0%	-	8.55	14	Sunflower oil				
9	EXA1SI	2.40%	0%	0%	-	8.55	15	Grape-seed oil				
10	EXA1SI	0%	1.20%	0%	-	8.55	16	Soybean oil				
11	EXA1SI	0%	2.40%	0%	-	8.55	17	Corn-seed oil				
12	EXA1SI	0%	0%	2.40%	-	8.55	18	Olive oil				

Table 2 Enthalpy change, H , induction time (IT) and peak time (PT) of isothermal freezing at 2.9°C

Sample no.	$H/J\text{ g}^{-1}$	IT/h	PT/h
2	21	7	20
3	22	7	19
6	24	15	35
7	26	9.5	15
8	21	11	17
9	25	7	17
10	24	11	17
11	23	11.5	20
12	23	6.5	12

by flame. Its mass is obtained by weighing. The measured quantities are: the complex heat capacity, the enthalpy of freezing calculated from the curve after base-line subtraction, the transition temperatures as observed in the cooling and heating runs. The calorimeter, the measuring procedures and data analysis are reported in [20].

DSC measurements

The measurements in the wide temperature range (-40)–(+50)°C have been performed with DSC 7 by PerkinElmer, after the standard calibration procedure, at a scanning rate of 10°C min⁻¹; the sample mass was typically 5 mg. Measurements were carried out under nitrogen, purity grade UPP.

Results

To compare extra-virgin olive oil (EVOO) with other edible oils and to put in evidence the sensitivity of the calorimetry as technique suitable for screening the oil identity, the first experiments were performed with the DSC, at the scanning rate of 10°C min⁻¹, to study the liquid↔solid phase transition of few oils, marked as ‘commercial edible oils’ in Table 1. The freezing curves of these oils are in Fig. 1A. The curve of the EVOO sample is characterized, in the explored temperature range, by a large crystallization peak at low temperature, which is absent in the other edible oils. Minor differences allow distinguishing also among them. In Fig. 1B are shown the differences induced in EVOO freezing curve by the addition of 25% of sunflower oil. The crystallization peak is reduced and shifted to low temperature and the effect is so large that it seems possible to pick out also the addition of a few per cent of seed oil to EVOO. These and other features of the freezing curve are particularly promising for a first screening of edible oils and their mixture identity. Thus our attention, in agreement with previous at-

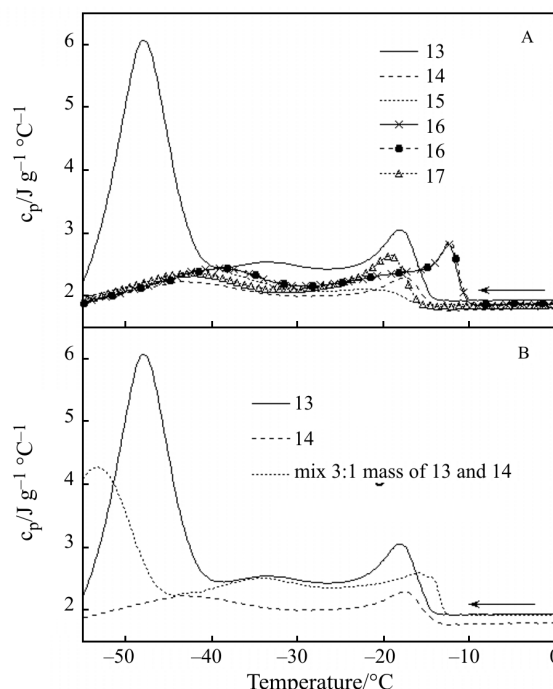


Fig. 1 DSC traces at cooling rate of 10°C min⁻¹. Entries refer to Table 1. A – commercial edible oils; the good reproducibility of the measurements is shown by the two runs performed on the same sample, no. 16; B – comparison between one extra-virgin olive oil, one seed oil and a mixture of the two at 25% of the seed oil

tempts reported in the literature [4, 10–12], is being mainly paid to the freezing process.

In Figs 2A and B are shown the freezing and melting curves of Tuscan EVOOs of different geographic origin (samples 1, 2, 3, 5, 6 of Table 1), together with a commercial EVOO (13) and a sample labelled ‘olive oil’ (18), obtained with the DSC, at the scanning rate of 10°C min⁻¹. The two commercial oils show evident differences in their DSC traces, mainly above 0°C. Indeed the second melting peak is strongly reduced.

The freezing kinetics of 9 samples was studied at 2.9°C with the TAM calorimeter. The experimental isotherms (heat flow vs. time) of pure EVOO of different origin and of defected oil samples from the same mother EVOO are shown in Fig. 3. The numbers near each curve identify the samples according to Table 1. Each oil sample freezes in a particular way, after an induction time, IT , needed to allow for the nucleation of the TAG polymorphs. IT varies widely in particular for defective oils (Fig. 3B).

In these experimental conditions it was observed that the IT value was not reproduced in the successive runs performed on the same sample, after it was melted at room temperature and then kept at this temperature also for long times.

A systematic study on the origin of this non-reproducibility was performed and the results are

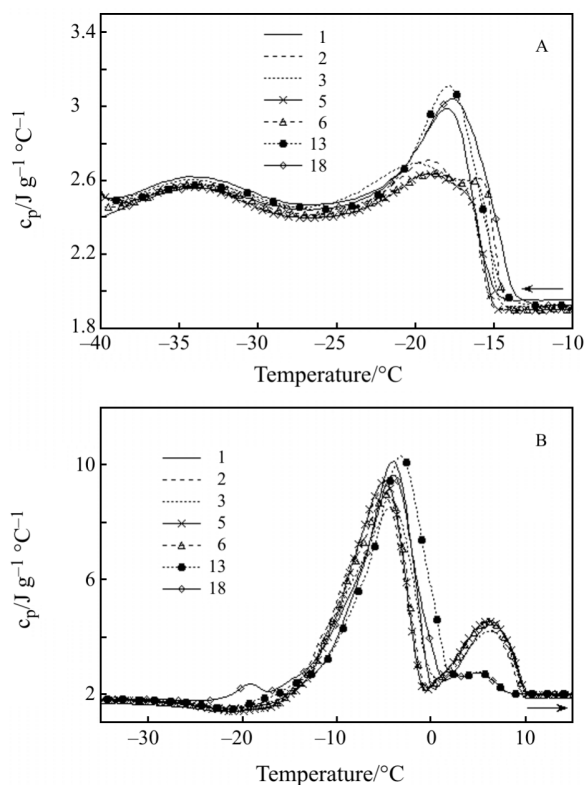


Fig. 2 DSC runs at the scanning rate of $10^\circ C\ min^{-1}$ of 5 Tuscan extra-virgin olive oils and two commercial oils. Entries refer to Table 1. A – the first freezing peak; B – melting

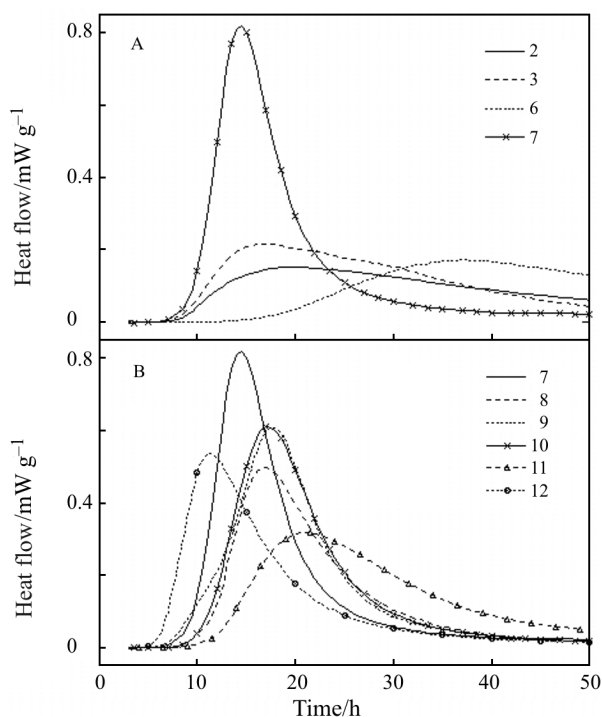


Fig. 3 Heat flow vs. time in isothermal calorimeter at $2.9^\circ C$ for the solidification of oils. Entries as in Table 1. A – four Tuscan extra-virgin olive oils; B – five defective oils

collected in Fig. 4. Curve labelled 2 represents the first freezing of the EVOO sample no. 2 at $2.9^\circ C$. The same sample was then melted at $18^\circ C$. After a storage time of 1 h at that temperature the sample was loaded again in the TAM calorimeter for the second run and the result is the curve 2a. The curve 2b was obtained by increasing the storage time at $18^\circ C$ up to 10 h. The effect induced by mechanical stirring (curve 2d), 5 min sonication at room temperature (curve 2c), and storage of the sample at $50^\circ C$ for 10 min (curve 2e), are also shown in Fig. 4.

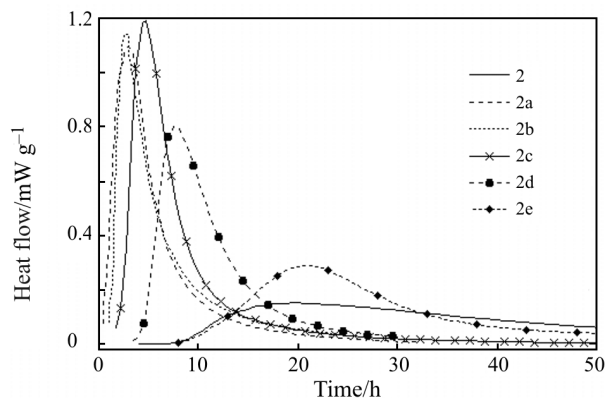


Fig. 4 Heat flow for solidification at $2.9^\circ C$ of sample no. 2 after these treatments: original sample (2), the sample melted at $18^\circ C$ (2a), melted and stored at $18^\circ C$ for 10 h (2b), melted and undergone to mechanical stirring (2c), melted and undergone to sonication for 5 min (2d), melted and heated to $50^\circ C$ for 10 min (2e)

To investigate the early freezing jump present in Fig. 1A between (-10) – $(-20)^\circ C$, we studied the freezing process with MASC at the temperature scanning rate, β of $0.25^\circ C\ min^{-1}$. The experimental results are in Fig. 5A. The beginning of the freezing, as marked by the intercept of the tangent in the flex point of the first peak with the base-line, occurs at this low β in the temperature range (-13) – $(-10)^\circ C$ (see the enlarged view in Fig. 5B). The label of each curve has the above declared meaning.

The melting curves, obtained for each sample after an isotherm of one hour at $-26^\circ C$, are in Fig. 6A. They show two peaks. The first one at lower T shows also a fine superimposed structure and occurs at a temperature (FMPT, first melting peak temperature) in the interval (-7) – $(-5.5)^\circ C$.

An enlargement of the decreasing part of the second melting peak is in Fig. 6B. In the melting curves is also present a small peak near $0^\circ C$, not visible in this figure, from which it is possible to calculate the amount of water present in the oil samples. The melting end (ME) occurs in the interval 10.7 – 11.1 h.

For a better understanding of the freezing process and the growth kinetics of the polymorphous

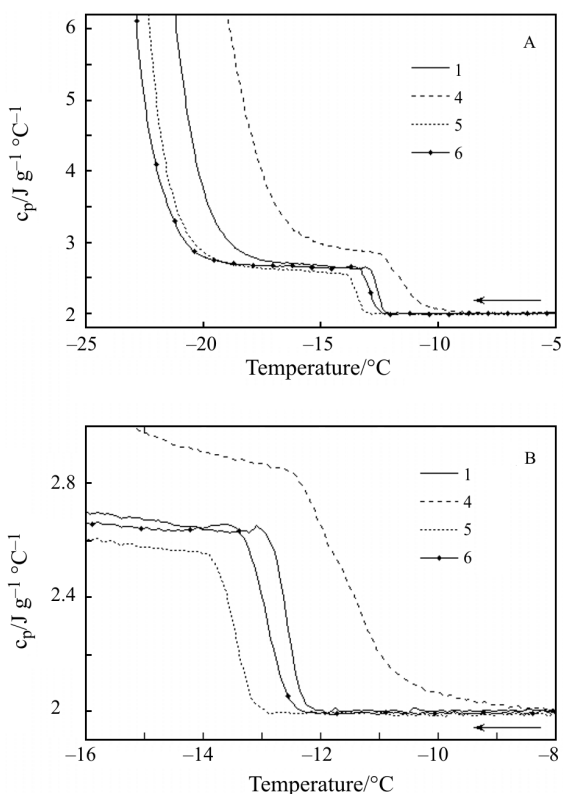


Fig. 5 Apparent specific heat, c_p , vs. T during cooling runs performed with MASC at $0.25^\circ\text{C min}^{-1}$. Entries as in Table 1. A – full curves. B – enlargement of the first freezing peaks

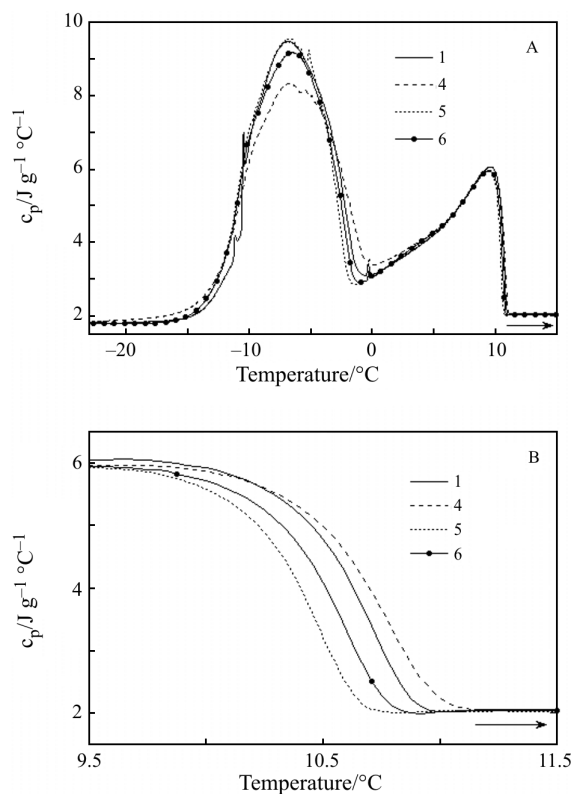


Fig. 6 Apparent specific heat, c_p , vs. T during heating runs performed with MASC at $0.25^\circ\text{C min}^{-1}$. Entries as in Table 1. A – full curves. B – enlargement of the last melting peaks

TAG crystals, MASC was also used with the following temperature–time profile: *i*) a single sample was firstly heated up to 50°C for 10 min for destroying local structures in the liquid, (this protocol was applied by Adhvaryu *et al.* [3] and confirmed by our results in Fig. 4, where the IT value was reproduced only after this sample treatment); *ii*) the sample was loaded in the calorimetric cell at $T = -25^\circ\text{C}$ and the freezing was monitored isothermally until the completion of the process; *iii*) finally, the sample was heated at the rate of $0.25^\circ\text{C min}^{-1}$ and the melting monitored. The above cycle was repeated with the increase of the isothermal freezing temperature by steps of 5°C each time, until the isotherm of the last cycle was at 0°C . The freezing isotherms are in Fig. 7.

In Fig. 8 are shown the heat flow, dH/dt , the enthalpy of freezing, H , the real, C'_p , and imaginary C''_p , components of the complex heat capacity, $C^* = C'_p + iC''_p$, measured with temperature modulation. The measurements were performed with a modulation period of 300 s, modulation amplitude of 0.5°C , at the mean temperature of -10 , -5 and 0°C .

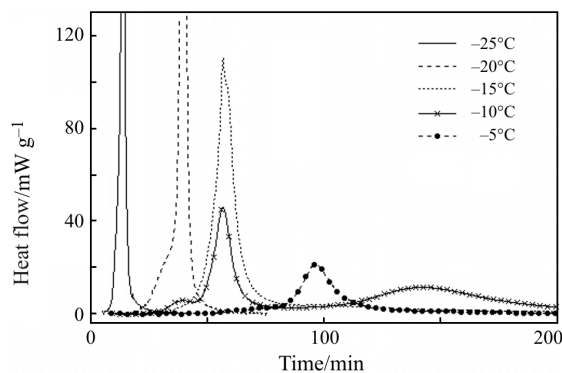


Fig. 7 Five isothermal freezing curves of a single sample (no. 6 of Table 1), monitored with MASC at temperatures from -25 to -5°C in steps of 5°C

Discussion

The ability of calorimetry to screen different edible oils and to put in evidence adulteration of EVOO by addition of low cost edible oils is evident in Figs. 1A and B. DSC calorimetry is also able to discriminate (Fig. 2) among the certified Tuscan EVOOs and the

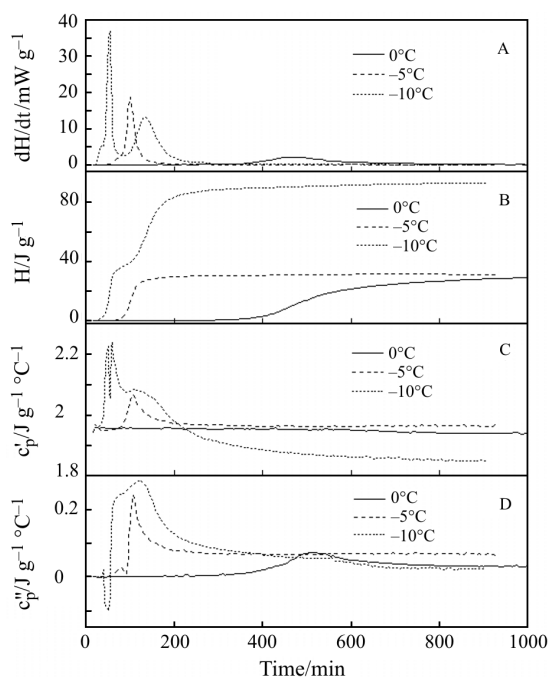


Fig. 8 Heat flow, dH/dt , freezing enthalpy, H , real C'_p and imaginary, C''_p , parts of the heat capacity (panel A, B, C and D, respectively), for sample no. 6. The quantities were measured simultaneously by MASC in the modulated temperature mode (modulation period=300 s; modulation amplitude=0.5°C), at the mean temperatures: -10, -5, 0°C

commercial EVOO (sample 18) and the olive oil (sample 13).

The freezing curves recorded with DSC and MASC show essentially the same features even if with different level of details owing to the different sensitivity of the two calorimeters, particularly at low scanning rates. It is possible to select two temperatures related to the freezing process: the first one comes from the jump occurring between -10.3 and -13.1°C (Fig. 5B); the second one marks the big exothermic peak, wider than 10°C at $\beta=0.25^\circ\text{C min}^{-1}$. The first temperature is known as Wax Appearance Temperature (WAT) and it is relevant for mineral oil characterization [20]. At this temperature the viscosity of the liquid shows a rapid increase and the solidification starts with the nucleation of the TAG polymorphs [3, 4]. We have observed that this temperature is particularly dependent on the type of defects and also on the origin of the EVOO.

The results obtained with TAM calorimeter show how the investigated oil samples 'freeze' at 2.9°C. The integral of the freezing curve gives the enthalpy of the process and its calculated values range between 21 and 26 J g⁻¹ (Table 2).

Quantities which are strongly dependent on the type of defect and on the oil origin (Fig. 3 and Table 2) are: *i*) the IT values, measured by the intercept

of the tangent at the flex point of the freezing curve with the baseline, and *ii*) the time at which the curves reach the peak (PT). The two quantities vary between 7–16 h and between 12–35 h, respectively. Moreover, a relevant feature of the isothermal freezing at 2.9°C is the large non-reproducibility of the second run, performed after each sample was melted at room temperature. Indeed, both IT and PT are reduced differently (from 0 to 15 h depending on the sample) as if few ordered structures would be able to survive in the melt, thus promoting the nucleation process at 2.9°C.

Two experiments were planned for shading light on this 'crystal structure memory in the liquid'. The results are shown in Fig. 4. The same IT value was obtained only after storing the sample at 50°C for 10 min, even if the curve shows a different profile (compare curves 2 and 2e).

The isothermal freezing curves of a single sample at different subzero temperatures (Fig. 7) show a large peak with the exception of the curve at -10°C, in which three peaks are present: a small peak just at beginning of the process, the highest peak after about 60 min and a broad peak about 80 min later. Another feature common to the other curves is the shoulder in the low temperature side of the peak, with the exception of the curve at -15°C, in which a shoulder occurs in the decreasing side of the peak. The enthalpy of the isothermal freezing decreases with the increasing of the temperature, indicating that the process cannot attain the completion at temperatures higher than -10°C, as can be extrapolated from the data in Table 3. The isothermal freezing at -10°C shows other anomalies both in the enthalpy value and in the induction time. A deeper investigation near this temperature is very promising for a better understanding of the nucleation process of the TAG polymorphs and for obtaining further parameters sensible to the EVOO quality. This study is in progress.

The results from modulated temperature calorimetry in Fig. 8 put in evidence that at -10, -5 and 0°C further information is contained in the C'_p curve. It is evident that the 'solid phase' grown at -5 and 0°C have a heat capacity higher than that of the liquid one.

Table 3 Temperature, enthalpy change, H , induction time (IT) and peak time (PT) of isothermal freezing of sample no. 6

$T/^\circ\text{C}$	$H/\text{J g}^{-1}$	IT/min	PT/min
-25	82	9	14
-20	83	22	40
-15	85	33	57
-10	92	28*	40/57/135
-5	32.2	53	97
0	22.8	162	295

*measured at the first peak

This means that the solid phases are evidently not normal crystalline phases.

The heat flow curve at -10°C shows three peaks and the same profile given by the unmodulated isothermal calorimetry (Fig. 7), and the C_p behaviour is normal. We are likely in presence of three cohabitant crystalline structures or a mixing of liquid-solid and solid-solid transitions towards the more stable polymorphous phases, as observed for cocoa butter [23]. The melting curve of the sample shows only two peaks as the curves in Figs 2B and 6A do. This evidence also supports the occurrence of solid-solid transitions in the sample.

Conclusions

The freezing and melting of oils are physical processes strongly affected by the size, type and concentration of the molecules present in the liquid phase. The calorimetric curves and data here reported, even if they represent only a part of the programmed measurements, outline that the nucleation kinetics, the growth rate of the polymorphs in which TAGs crystallize and the melting of the solid samples are, in particular, very rich of information. It is, indeed, possible to define numerous parameters that are correlated to a different extent with origin, type of cultivars, and defects of EVOOs. A particular EVOO could be therefore identified by a set of parameters (for example *IT*, *PTs*, *H*, *WAT*, C_p , *ME*, *FMPT*, and possibly others deducible from the fine details of the first melting peak and isothermal freezing observed with modulated calorimetry), that is by a sort of identification label, or 'fingerprint' [10], settled on according to an agreed protocol for the EVOO of each production region and harvest.

Each calorimetric technique and/or operation mode is useful in itself: DSC can discriminate in short time between olive oil and other edible oils and also between commercial and guaranteed origin EVOOs; the high sensitivity isothermal calorimetry, TAM, is time consuming but is able to provide parameters as *IT* and *H* that are particularly sensible to defects and origin of EVOOs; MASC, with its temperature modulated and adiabatic (not yet applied here) measurements, in addition to the modes of the other two calorimeters, widens the research field to a detailed study of the crystallization process.

Summing up, information collected with multimode calorimetry is very promising for screening quality and origin of EVOOs.

The present outline of the performances of calorimetry must be followed by a systematic work for correlating the numerous parameters with the more relevant qualities of the typical Tuscan EVOO's, defining a sensitivity scale for identifying the main

commercial frauds, etc. We hope that the integration of data from multimode calorimetry with those from artificial nose technique and the development of a suitable data analysis will help devise a protocol for a powerful screening of quality and origin of olive oils.

References

- 1 'Olive Oil from the Tree to the Table' second ed., A. Kiritsakis, Food and Nutrition Press, Inc., Trumbull, Connecticut (USA) 1998.
- 2 A. Kiritsakis and W. W. Christie, 'Analysis of Edible Oils' in Handbook of Olive Oil, J. Harwood and A. Aparicio Eds., An Aspen Publication (USA) 129–158 (2000).
- 3 A. Adhvaryu, S. Z. Erhan and J. M. Perez, *Thermochim. Acta*, 395 (2003) 191.
- 4 K. Sato, *Chem. Eng. Sci.*, 56 (2001) 2255.
- 5 C. G. Bilalderis, *Food Chem.*, 10 (1983) 239; D. Dollimore, *Anal. Chem.*, 68 (1996) 63R.
- 6 M. Cabrera, *Grasas y Aceites*, 43 (1992) 259.
- 7 H. Gloria and J. M. Aguilera, *J. Agric. Food Chem.*, 46 (1998) 1363.
- 8 E. Vittadini, J. H. Lee, N. G. Frega, D. B. Min and Y. Vodovotz, *J. Am. Oil Chem. Soc.*, 80A (2003) 533.
- 9 A. Kanavouras and S. Selke, *Eur. J. Lipid Sci. Technol.*, 106 (2004) 359.
- 10 S. M. Dyszel, *Thermochim. Acta*, 57 (1982) 209.
- 11 S. M. Dyszel and S. K. Baish, *Thermochim. Acta*, 212 (1992) 39.
- 12 S. M. Dyszel, *Thermochim. Acta*, 284 (1996) 103.
- 13 G. Litwinienko, A. Daniluk and T. Kasprzycza-Guttman, *J. Am. Oil Chem. Soc.*, 76 (1999) 655.
- 14 C. P. Tan and Y. B. Che Man, *J. Am. Oil Chem. Soc.*, 76 (1999) 1047.
- 15 G. Hugo and J. M. Aguilera, *J. Agric. Food Chem.*, 46 (1998) 1363.
- 16 C. P. Tan, Y. B. Che Man, J. Selamat and M. S. A. Yussoff, *Chemistry*, 76 (2002) 385.
- 17 J. Dweck, C. M. S. Sampaio, *J. Therm. Anal. Cal.*, 75 (2004) 385.
- 18 J. C. O. Santos, I. M. G. Santos, M. M. Conceição, S. L. Porto, M. F. S. Trindade, A. G. Souza, S. Prasad, V. J. Fernandes and A. S. Araújo, *J. Therm. Anal. Cal.*, 75 (2004) 419.
- 19 A. Banti, N. Minnaja, E. Colle, E. Dalcanale, L. Scarselli, A. Tessa and L. Sensi, Proceedings of the 10th Italian Conference on Sensors and Microsystems, 2005, to be published.
- 20 G. Salvetti, C. Cardelli, C. Ferrari and E. Tombari, *Thermochim. Acta*, 364 (2000) 11.
- 21 Z. Jiang, J. M. Hutchinson and C. T. Imrie, *Fuel*, 80 (2001) 367.
- 22 A. Raemy, I. Froelicher and J. Loeliger, *Thermochim. Acta*, 114 (1987) 159.
- 23 D. Fessas, M. Signorelli and A. Schiraldi, *J. Therm. Anal. Cal.*, 82 (2005) 691.

DOI: 10.1007/s10973-005-7184-8